



CHORUS

This is the accepted manuscript made available via CHORUS. The article has been published as:

Quantum calculation of inelastic neutron scattering spectra of a hydrogen molecule inside a nanoscale cavity based on rigorous treatment of the coupled translation-rotation dynamics

Minzhong Xu, Lorenzo Ulivi, Milva Celli, Daniele Colognesi, and Zlatko Bačić

Phys. Rev. B **83**, 241403 — Published 15 June 2011

DOI: [10.1103/PhysRevB.83.241403](https://doi.org/10.1103/PhysRevB.83.241403)

Quantum calculation of inelastic neutron-scattering spectra of a hydrogen molecule inside a nanoscale cavity based on rigorous treatment of the coupled translation-rotation dynamics

Minzhong Xu,² Lorenzo Ulivi,³ Milva Celli,³ Daniele Colognesi,³ and Zlatko Bačić*^{1,2}

¹*State Key Laboratory of Precision Spectroscopy and Department of Physics,
Institute of Theoretical and Computational Science,*

East China Normal University, Shanghai 200062, China

²*Department of Chemistry, New York University, New York, NY 10003*

³*Consiglio Nazionale delle Ricerche, Istituto dei Sistemi Complessi,
Via Madonna del Piano 10, I-50019, Sesto Fiorentino, Italy*

Abstract

We present a quantum methodology for the calculation of the inelastic neutron scattering (INS) spectra of an H₂ molecule confined in a nanoscale cavity. Our approach incorporates the coupled 5D translation-rotation (T-R) energy levels and wave functions of the guest molecule. The computed INS spectra are highly realistic and reflect in full the complexity of the coupled T-R dynamics on the anisotropic potential energy surfaces of the confining environment. Utilizing this methodology we simulate the INS spectra of *p*- and *o*-H₂ in the small cage of the structure II clathrate hydrate and compare them with the experimental data.

PACS numbers: 78.70.Nx, 67.80.ff, 82.75.-z

* Electronic mail: zlatko.bacic@nyu.edu

Inelastic neutron scattering (INS) spectroscopy is an extremely valuable and widely used tool for investigating on a microscopic level the properties of hydrogen molecules confined inside the nanosize cavities of diverse host materials. Its remarkable power stems from two key features. One of them is the exceptionally large incoherent neutron scattering cross section of the proton, nearly two orders of magnitude greater than for any other nucleus. Therefore, in presence of a relevant concentration of protons, the bands in the spectra due to the host vibrational modes not involving hydrogen are typically quite small, making INS a highly selective probe of the dynamics of the encapsulated hydrogen molecules. The second unique feature of the INS is the ability of neutrons to induce nuclear spin transitions. This makes it possible to observe the rotational $\Delta J = 1$ transitions, e.g., $J = 0 \rightarrow 1$ of *para*-H₂ (*p*-H₂) and $J = 1 \rightarrow 2$ of *ortho*-H₂ (*o*-H₂), which are forbidden in optical, infrared (IR) and Raman spectroscopy of H₂ since they involve the *ortho-para* conversion.

In recent years, the INS spectroscopy has been used to study the behavior of molecular hydrogen encapsulated in a wide variety of materials, including fullerenes^{1,2}, clathrate hydrates^{3,4}, metal-organic frameworks (MOFs)⁵⁻⁷, and zeolites^{8,9}. INS spectra are rich in information about the specifics of binding and dynamics of the entrapped H₂, and its interactions with the host materials. However, until recently, only a fraction of the information encoded in the INS spectra could be extracted with the low-dimensional theoretical approaches that have been used to analyze them. Thus, for the INS spectra of H₂ in MOFs, tentative assignments of the peaks to the H₂ rotational excitations at different binding sites have been made using the eigenvalues of a single-parameter phenomenological model for the rotational potential^{5,6,9}. These assignments were uncertain and incomplete, as they left out the excitations of the H₂ center-of-mass (cm) translation. Similarly, the splitting of the $J = 1$ rotational state into a triplet, observed in the INS spectra of H₂ in the aza-thia-open-cage fullerene (ATOCF), was rationalized in terms of the eigenvalues of a model anisotropic rotational potential with three adjustable parameters¹. Recently, the INS spectra of H₂ in a MOF were assigned by comparison with the rotational and translational energy levels of the diatomic computed separately on the *ab initio*-calculated 2D angular and 1D radial potential energy surfaces (PESs), respectively¹⁰. The main weakness of all these approaches is that the rotation of H₂ is assumed to be decoupled from its cm translation. Moreover, no attempt was made to compute the INS intensities of the T-R transitions.

The three translational and the two rotational degrees of freedom of a nanoconfined H₂

molecule are in fact intricately coupled, as illustrated below. In a series of recent papers, we have initiated rigorous investigations of the quantum translation-rotation (T-R) dynamics of one or more hydrogen molecules encapsulated in the small^{11,12} and large cages^{13,14} of the structure II (sII) clathrate hydrate, and subsequently, inside the fullerenes C₆₀¹⁵⁻¹⁸, C₇₀^{16,17}, and ATOCF¹⁹. For H₂/HD/D₂ in the small cage of sII clathrate hydrate¹² and H₂ in ATOCF¹⁹, direct comparison between the T-R excitation energies from the quantum 5D calculations and the measured INS spectra^{1,3} proved very useful for the interpretation of the observed rotational and translational excitations.

The assignment of the measured INS spectra, especially at higher energies, would be made with much more confidence if in addition to the energies of the T-R transitions one could calculate accurately their intensities as well, and compare them with the experimental data. But, in the few calculations of the INS spectra of H₂ in zeolites^{20,21}, the translational motion of H₂ was treated classically, which is inadequate for the low temperatures of interest, and the H₂ rotations quantum mechanically. Another major shortcoming of this mixed quantum-classical approach is its inability to account for the translational excitations. The quantum treatments of the INS from molecular systems, intended for the weakly interacting molecular hydrogen in the solid^{22,23}, liquid^{24,25}, and gas phase²⁴, make the approximation that the translational and rotational motions of the molecule are decoupled.

Neglecting the T-R coupling when simulating the INS spectra of an H₂ molecule in a nanocage would result in two kinds of errors. (1) The energies of the calculated energy levels would be incorrect (for the PES employed), and so would be the transition energies. (2) Energy levels which arise solely because the T-R coupling lifts certain level degeneracies would be missing entirely. As one example of (1), we consider the rotational $j = 1$ triplet of H₂ in the small cage of sII hydrate, whose degeneracy is lifted completely by the angular anisotropy of the PES^{3,11,12}. The $j = 1$ triplet, by itself or in combination with translational excitations, figures prominently in the INS spectra, as shown later in this paper. Based on our quantum 5D calculations¹², the splitting of the $j = 1$ triplet in the ground translational state is 19.2 cm⁻¹. With one quantum of excitation in the translational z mode¹² ($v_z = 1$), the $j = 1$ splitting increases to 21.9 cm⁻¹; it increases further to 24.1 cm⁻¹ for $v_z = 2$, and 26.4 cm⁻¹ for $v_z = 3$. Thus, in going from $v_z = 0$ to $v_z = 3$, the $j = 1$ triplet splitting grows from 19.2 to 26.4 cm⁻¹, an increase of 37.5% caused by the T-R coupling. The calculations *without* the T-R coupling would yield the $j = 1$ triplet splitting which

is *constant*, independent of the translational excitation. Therefore, in the corresponding simulated INS spectra, the transitions involving the $j = 1$ triplet would appear at energies significantly different from those computed with the T-R coupling included. An example of (2) is provided by $\text{H}_2@C_{60}$. Our quantum 5D calculations predicted that translationally *and* rotationally excited level $n = 1, j = 1$ is split into *three* levels, due *solely* to the T-R coupling^{15,16,18}. The predicted triplet was observed in both the INS² and IR spectra²⁶ of $\text{H}_2@C_{60}$. In contrast, the calculations assuming *no* T-R coupling would give a *single* $n = 1, j = 1$ level, since both the translational fundamental ($n = 1$) and the $j = 1$ rotational level of H_2 in C_{60} by themselves remain triply degenerate¹⁵. Thus, the INS spectra of $\text{H}_2@C_{60}$ computed without the T-R coupling would be *qualitatively* wrong and incomplete. These and many other examples illustrate the importance of including the T-R coupling in the calculations of the INS spectra of nanoconfined molecules.

In this paper we present the quantum methodology for calculating the INS spectra for H_2 inside a nanocavity i.e., the energies of the T-R transitions and their intensities, which for the first time incorporates rigorously the translation-rotation interactions. The computed spectra faithfully mirror the complexity of the “rattling” dynamics of the molecule confined in an anisotropic environment. This uniquely high degree of realism and detail in simulating the INS spectra is not achievable by the approaches in the literature. It is made possible by our ability to compute accurately the fully coupled quantum 5D T-R energy levels and wave functions of the entrapped molecule on the 5D intermolecular PES^{11,12,15,16} and, as shown here, use them as input for calculating the spectra.

Only a brief summary of the theory is given in this paper, while a detailed description will be presented elsewhere²⁷. As in all the quantum treatments of the INS spectroscopy, our starting point is the standard expression for the neutron scattering double differential cross section in the first Born approximation^{22,28}:

$$\frac{d^2\sigma}{d\Omega d\omega} = \frac{k'}{k} S(\vec{\kappa}, \omega), \quad S(\vec{\kappa}, \omega) = \sum_i p_i \sum_f |M_f^i|^2 \delta[\omega - (\epsilon_f - \epsilon_i)/\hbar], \quad (1)$$

$$M_f^i = \sum_n \langle f | \hat{b}_n \exp(i\vec{\kappa} \cdot \vec{r}_n) | i \rangle. \quad (2)$$

Here $|i\rangle$ is the initial state of the scattering molecular system with the energy ϵ_i , p_i its statistical weight, $|f\rangle$ the final state with the energy ϵ_f , $\vec{\kappa} = \vec{k} - \vec{k}'$; \vec{k} and \vec{k}' the wave vectors of the incident and the scattered neutrons, respectively, $\hbar\omega = E - E' = \hbar^2(k^2 - k'^2)/(2m)$, m the neutron mass; \hat{b}_n is the scattering length operator, \vec{r}_n the position of nucleus n . For

a single nucleus n , the scattering operator reads: $\hat{b}_n = A + B \frac{\vec{\sigma}}{2} \cdot \vec{i}_n$, where $\frac{\vec{\sigma}}{2}$ represents the neutron spin and \vec{i}_n the nuclear spin. For the proton, $A = -0.374 \cdot 10^{-14}$ m and $B = 5.836 \cdot 10^{-14}$ m²⁸; they are related to the coherent, σ_c , and incoherent, σ_i , scattering cross sections of the proton: $\sigma_c = 4\pi A^2$, $\sigma_i = 3\pi B^2/4$. The initial and final states of the scattering molecular system in Eqs. (1) and (2) can be written in the product form

$$|i\rangle = |I_i\rangle |\Psi_i(\vec{r}_1, \vec{r}_2, \dots, \vec{r}_n)\rangle \quad |f\rangle = |I_f\rangle |\Psi_f(\vec{r}_1, \vec{r}_2, \dots, \vec{r}_n)\rangle. \quad (3)$$

$|I_\tau\rangle$ and $|\Psi_\tau(\vec{r}_1, \vec{r}_2, \dots, \vec{r}_n)\rangle$ ($\tau = i, f$) are the nuclear spin and spatial wave functions.

We now consider a single nanoconfined H₂ molecule; both the molecule and the nanocage are taken to be rigid. The position of the n th H atom is given by $\vec{r}_n = \vec{R}_{cm} + (-1)^n \vec{\rho}/2$, $n = 1, 2$, where \vec{R}_{cm} is the position vector of the cm of H₂ and $\vec{\rho}$ is the vector connecting the two H atoms. To calculate $S(\vec{\kappa}, \omega)$ defined by Eqs. (1) and (2), for the spatial components of the states $|i\rangle$ and $|f\rangle$ in Eq. (3) we use the accurately computed 5D wave functions $|\Psi_\tau^{5D}(\vec{R}_{cm}, \theta_\rho, \phi_\rho)\rangle$ and the corresponding energy levels ϵ_τ ($\tau = i, f$) of the 5D T-R Hamiltonian of the caged H₂ molecule^{11,12,15,16}; θ_ρ, ϕ_ρ specify the orientation of H₂ in the cage. In the following, $|\Psi_\tau^{5D}(\vec{R}_{cm}, \theta_\rho, \phi_\rho)\rangle$ are denoted as $|\Psi_\tau^{5D}\rangle$. One obtains²⁷

$$S(\vec{\kappa}, \omega) = \sum_i p_i \sum_f \sigma_{I_i \rightarrow I_f} \left| \langle \Psi_f^{5D} | \exp(i\vec{\kappa} \cdot \vec{R}_{cm}) \sin(\vec{\kappa} \cdot \vec{\rho}/2) | \Psi_i^{5D} \rangle \right|^2 \delta[\omega - (\epsilon_f - \epsilon_i)/\hbar], \quad (4)$$

where $\sigma_{I_i \rightarrow I_f}$ is the spin-dependent neutron scattering cross section. This equation applies to p -H₂ \rightarrow o -H₂ and o -H₂ \rightarrow p -H₂ transitions. For p -H₂ \rightarrow p -H₂ and o -H₂ \rightarrow o -H₂ transitions, $\sin(\vec{\kappa} \cdot \vec{\rho}/2)$ in Eq. (4) is replaced with $\cos(\vec{\kappa} \cdot \vec{\rho}/2)$ ²⁷.

In the 5D basis, the T-R eigenvectors $|\Psi_\tau^{5D}\rangle$ are expanded as $|\Psi_\tau^{5D}\rangle = \sum_{\alpha\beta\gamma jm} {}^{5D}A_{\alpha\beta\gamma jm, \tau}^{xyz\theta\phi} |X_\alpha\rangle |Y_\beta\rangle |Z_\gamma\rangle |jm\rangle$ ²⁹. $\{|X_\alpha\rangle |Y_\beta\rangle |Z_\gamma\rangle\}$ is the 3D direct product discrete variable representation (DVR)³⁰ basis in the Cartesian x, y, z coordinates (the so-called sinc DVR³¹); it is labeled by the grid points $\{X_\alpha\}$, $\{Y_\beta\}$, and $\{Z_\gamma\}$, at which the respective DVR basis functions are localized. The angular basis $\{|jm\rangle\}$ are the (modified) spherical harmonics²⁹. The expression $\exp(i\vec{\kappa} \cdot \vec{\rho}/2) = \sum_{lm} i^l 4\pi j_l \left(\frac{\kappa\rho}{2}\right) Y_{lm}^*(\theta_{\vec{\kappa}}, \phi_{\vec{\kappa}}) Y_{lm}(\theta_\rho, \phi_\rho)$ ³² is employed, of which $\cos(\vec{\kappa} \cdot \vec{\rho}/2)$ and $\sin(\vec{\kappa} \cdot \vec{\rho}/2)$ above are real and imaginary parts, respectively.

The spatial component of Eq. (4) can be rewritten as:

$$\begin{aligned} \langle \Psi_f^{5D} | \exp(i\vec{\kappa} \cdot \vec{R}_{cm}) \sin(\vec{\kappa} \cdot \vec{\rho}/2) | \Psi_i^{5D} \rangle &= \sum_{\alpha\beta\gamma jmj'm'} {}^{5D}A_{\alpha\beta\gamma j'm', f}^{xyz\theta\phi} {}^{5D}A_{\alpha\beta\gamma jm, i}^{xyz\theta\phi} \quad (5) \\ &\times \langle j'm' | \sin(\vec{\kappa} \cdot \vec{\rho}/2) | jm \rangle \exp[i\kappa (\sin \theta_{\vec{\kappa}} \cos \phi_{\vec{\kappa}} X_\alpha + \sin \theta_{\vec{\kappa}} \sin \phi_{\vec{\kappa}} Y_\beta + \cos \theta_{\vec{\kappa}} Z_\gamma)], \end{aligned}$$

where $(\theta_{\vec{\kappa}}, \phi_{\vec{\kappa}})$ are the angles of $\vec{\kappa}$ ²⁷. As in Eq. (4), for $p\text{-H}_2 \rightarrow p\text{-H}_2$ and $o\text{-H}_2 \rightarrow o\text{-H}_2$ transitions, $\sin(\vec{\kappa} \cdot \vec{\rho}/2)$ in Eq. (5) is replaced with $\cos(\vec{\kappa} \cdot \vec{\rho}/2)$.

Eq. (5), together with expression for $S(\vec{\kappa}, \omega)$ in Eq. (4), permits the calculation of the INS spectra of a hydrogen molecule in an arbitrarily shaped (rigid) nanocavity, and also their temperature dependence, provided that the quantum 5D T-R eigenstates have been computed. The accuracy of the simulated INS spectra is limited primarily by the quality of the 5D intermolecular PES employed; consequently, their comparison with the measured INS spectra provides a stringent test of the PES.

As a demonstration of the methodology described in this paper, we have calculated the INS spectra of p - and o -H₂ in the small cage of the sII clathrate hydrate. This system was the very first whose coupled quantum T-R dynamics was investigated in 5D¹¹. We revisited it soon¹², after the first INS spectra were reported for the binary D₂O clathrate with H₂ and perdeuterated tetrahydrofuran (THF-d₈) as guest molecules³. Since the large cages are all occupied by the THF-d₈, H₂ molecules can reside only in the small cages, one per cage³. A standard data reduction³³ was performed, as well as the correction for the self-absorption attenuation in the sample through an analytical approach³⁴. By measuring independently the THF-d₈-D₂O clathrate hydrate sample in an identical aluminum cell, but with no hydrogen, its signal was accurately subtracted from the spectra. Consequently, the reported experimental INS spectra are exclusively due to H₂ molecules in the small cages. Multiple scattering contributions from two or more inelastic scattering events were evaluated approximately and found to be negligible over the entire energy-transfer interval of interest.

The 5D PES, the quantum 5D T-R energy levels and wave functions used to compute the INS spectra were reported in Ref.¹². At 20 K, the temperature of the experiment, only the lowest rotational states $J = 0, 1$ are populated, and therefore are the only initial states considered in the calculations. The initial $J = 1$ level is split into three components by the angular anisotropy of the PES¹², and in the calculations their population is weighted by the Boltzmann distribution at 20 K. The theoretical intensities were calculated for the two momentum-transfer values corresponding to the two scattering angles, forward at 42.6° and backward at 137.7°, available on TOSCA neutron spectrometer³⁵. The results presented correspond to the averages of the intensities calculated, and measured, at these two angles. Since the experimental data were taken from powdered samples, the computed INS spectra are also averaged over all possible orientations of the nanocages²⁷.

The simulated INS spectra of a hydrogen molecule in the small cage are displayed for p -H₂ in Fig. 1 and for o -H₂ in Fig. 2; the corresponding experimental spectra are shown for comparison. In both figures, two types of calculated spectra are shown, stick spectra at the top and those obtained by convolving with the instrumental resolution function appropriate for TOSCA spectrometer at the bottom. In the quantity $S(Q, \omega)$ on the vertical axis, $Q = |\vec{k}| = |\vec{k} - \vec{k}'|$ is the norm of the momentum transfer vector. The spectra computed for p - and o -H₂, based on the known scattering cross sections for the proton, have the same (arbitrary) units on the vertical axis. A single normalization constant was used to link the intensities of the INS spectra measured for both p - and o -H₂ to their respective theoretical counterparts. The transitions originating from the rotational states $J_i = 0, 1$ are labeled by their final rotational states J_f and by the translational quantum numbers introduced previously¹²; v_{xy} denotes the total number of quanta in the x - and y -mode excitations, while v_z is the Cartesian quantum number of the z -mode excitations¹².

Even a cursory comparison of the calculated and measured INS spectra in Figs. 1 and 2 shows that each observed band corresponds to a large number of unresolved individual T-R transitions. This signals that in the absence of accurate calculations the interpretation of the spectra is bound to be inconclusive. The spectrum of p -H₂ in Fig. 1 contains the rotationally inelastic $J = 0 \rightarrow 1$ transition, alone and in combination with various translational excitations having one or more quanta in different modes. The $J = 0 \rightarrow 1$ transition (1, 0, 0) itself, around 14 meV, is split into a triplet by the angular anisotropy of the PES. Its radial anisotropy causes the triplet splitting of the translational fundamental, (1, 1, 0) and (1, 0, 1), giving rise to the band between 20-30 meV. This band actually consists of nine transitions, three one-quanta excitations built on each of the three $J = 1$ sublevels. The INS spectrum of o -H₂ shown in Fig. 2 arises from both the rotationally elastic $J = 1 \rightarrow 1$ and the inelastic $J = 1 \rightarrow 2$ transitions, and a variety of translational excitations built on them. The number of discrete transitions in the stick spectrum of o -H₂ is much greater than for p -H₂, because in the former they originate from each of the three $J = 1$ sublevels. The spectrum of o -H₂ is also more complicated, and would be virtually impossible to assign with confidence without the high-level quantum simulation, since many of the bands contain overlapping contributions from both $J = 1 \rightarrow 1$ and $J = 1 \rightarrow 2$ transitions, combined with the translational excitations. The calculated and measured INS spectra show a remarkable overall agreement. The residual differences regarding the energies and widths of some

peaks have several possible causes, e.g., certain deficiencies in the PES and the fact that the H atoms of the framework water molecules are configurationally disordered, while the calculations are done for a single hydrogen-bonding configuration.

In conclusion, we have presented a novel methodology for the quantum calculation of the INS spectra of H₂ molecule in nanoscale confinement, which utilizes the 5D T-R eigenstates of the guest molecule. The computed spectra are highly realistic to a degree not achieved previously, and fully capture the complexity arising from the coupled T-R dynamics of H₂ entrapped in an anisotropic nanocavity. Applications to the INS spectra of H₂ and HD in C₆₀² and MOFs⁵ are in progress. Our approach is readily extended to the INS spectra of confined polyatomic molecules such as CH₄, whose 6D T-R eigenstates in methane hydrate we have calculated³⁶. The developments in this direction are under way in our group.

The authors at NYU thank the NSF for its partial support of this research through the Grant CHE-1112292. The computational resources at NYU used in this work were funded in part by the NSF MRI Grant CHE-0420810. The authors at NYU acknowledge stimulating conversations with Dr. Juergen Eckert (UC-Santa Barbara). This work was also partially supported by the Italian Ministry of Instruction, University and Research (MIUR) under the project PRIN 2008 AFW2JS.

-
- ¹ A. J. Horsewill, K. S. Panesar, S. Rols, M. R. Johnson, Y. Murata, K. Komatsu, S. Mamone, A. Danquigny, F. Cuda, S. Maltsev, M. C. Grossel, M. Carravetta and M. H. Levitt, *Phys. Rev. Lett.* **102**, 013001 (2009).
- ² A. J. Horsewill, S. Rols, M. R. Johnson, Y. Murata, M. Murata, K. Komatsu, M. Carravetta, S. Mamone, M. H. Levitt, J. Y. -C. Chen, J. A. Johnson, X. Lei and N. J. Turro, *Phys. Rev. B* **82**, 081410(R) (2010).
- ³ L. Ulivi, M. Celli, A. Gianassi, A. J. Ramirez-Cuesta, D. J. Bull and M. Zoppi, *Phys. Rev. B* **76**, 161401(R) (2007).
- ⁴ K. T. Tait, F. Trouw, Y. Zhao, C. M. Brown and R. T. Downs, *J. Chem. Phys.* **127**, 134505 (2007).
- ⁵ J. L. C. Rowsell, J. Eckert and O. M. Yaghi, *J. Am. Chem. Soc.* **127**, 14904 (2005).
- ⁶ F. M. Mulder, T. J. Dingemans, H. G. Schimmel, A. J. Ramirez-Cuesta and G. J. Kearley, *Chem. Phys.* **351**, 72 (2008).
- ⁷ P. D. C. Dietzel, P. A. Georgiev, J. Eckert, R. Blom, T. Strässle and T. Unruh, *Chem. Commun.* **46**, 4962 (2010).
- ⁸ P. A. Georgiev, A. Albinati, B. L. Mojct, J. Ollivier and J. Eckert, *J. Am. Chem. Soc.* **129**, 8086 (2007).
- ⁹ J. M. Nicol, J. Eckert and J. Howard, *J. Phys. Chem.* **92**, 7117 (1988).
- ¹⁰ L. Kong, G. Román-Peréz, J. M. Soler and D. C. Langreth, *Phys. Rev. Lett.* **103**, 096103 (2009).
- ¹¹ M. Xu, Y. Elmatad, F. Sebastianelli, J. W. Moskowitz and Z. Bačić, *J. Phys. Chem. B* **110**, 24806 (2006).
- ¹² M. Xu, F. Sebastianelli and Z. Bačić, *J. Chem. Phys.* **128**, 244715 (2008).
- ¹³ M. Xu, F. Sebastianelli and Z. Bačić, *J. Phys. Chem. A* **113**, 7601 (2009).
- ¹⁴ A. Witt, F. Sebastianelli, M. E. Tuckerman and Z. Bačić, *J. Phys. Chem. C* **114**, 20775 (2010).
- ¹⁵ M. Xu, F. Sebastianelli, Z. Bačić, R. Lawler and N. J. Turro, *J. Chem. Phys.* **128**, 011101 (2008).
- ¹⁶ M. Xu, F. Sebastianelli, B. R. Gibbons, Z. Bačić, R. Lawler and N. J. Turro, *J. Chem. Phys.* **130**, 224306 (2009).
- ¹⁷ F. Sebastianelli, M. Xu, Z. Bačić, R. Lawler and N. J. Turro, *J. Am. Chem. Soc.* **132**, 9826

- (2010).
- ¹⁸ S. Mamone, J. Y. -C. Chen, R. Bhattacharyya, M. H. Levitt, R. G. Lawler, A. J. Horsewill, T. Rõõm, Z. Bačić and N. J. Turro, *Coord. Chem. Rev.* **255**, 938 (2011).
- ¹⁹ S. Ye, M. Xu, Z. Bačić, R. Lawler and N. J. Turro, *J. Phys. Chem. A* **114**, 9936 (2010).
- ²⁰ A. L. R. Bug and G. J. Martyna, *Chem. Phys.* **261**, 89 (2000).
- ²¹ J. A. MacKinnon, J. Eckert, D. F. Coker and A. L. R. Bug, *J. Chem. Phys.* **114**, 10137 (2001).
- ²² H. Stein, H. Stiller and R. Stockmeyer, *J. Chem. Phys.* **57**, 1726 (1972).
- ²³ D. Colognesi, M. Celli and M. Zoppi, *J. Chem. Phys.* **120**, 5657 (2004).
- ²⁴ J. A. Young and J. U. Koppel, *Phys. Rev.* **135**, A603 (1964).
- ²⁵ M. Zoppi, *Physica B* **183**, 235 (1993).
- ²⁶ S. Mamone, M. Ge, D. Hüvonen, U. Nagel, A. Danquigny, F. Cuda, M. C. Grossel, Y. Murata, K. Komatsu, M. H. Levitt, T. Rõõm and M. Carravetta, *J. Chem. Phys.* **130**, 081103 (2009).
- ²⁷ M. Xu, L. Ulivi, M. Celli, D. Colognesi and Z. Bačić (manuscript in preparation).
- ²⁸ S. W. Lovesey. *Theory of neutron scattering from condensed matter, Volume 1*. Oxford University Press, Oxford, (1984).
- ²⁹ S. Liu, Z. Bačić, J. W. Moskowitz and K. E. Schmidt, *J. Chem. Phys.* **103**, 1829 (1995).
- ³⁰ Z. Bačić and J. C. Light, *Annu. Rev. Phys. Chem.* **40**, 469 (1989).
- ³¹ D. T. Colbert and W. H. Miller, *J. Chem. Phys.* **96**, 1982 (1992).
- ³² D. M. Brink and G. R. Satchler. *Angular momentum*. Clarendon Press, Oxford, (1968).
- ³³ P. C. H. Mitchell, S. F. Parker, A. J. Ramirez-Cuesta and J. Tomkinson. *Vibrational Spectroscopy with Neutrons*. World Scientific, Singapore, (2005).
- ³⁴ A. K. Agrawal, *Phys. Rev. A* **4**, 1560 (1971).
- ³⁵ D. Colognesi, M. Celli, F. Cillico, R. J. Newport, S. F. Parker, V. Rossi-Albertini, F. Sacchetti, J. Tomkinson and M. Zoppi, *Appl. Phys. A* **62**, 64 (2002).
- ³⁶ I. Matanović, M. Xu, J. W. Moskowitz, J. Eckert and Z. Bačić, *J. Chem. Phys.* **131**, 224308 (2009).

FIG. 1: The calculated and measured INS spectra of p -H₂ in the small cage of sII clathrate hydrate. The top figure shows the stick spectrum, while the one convolved with the instrumental resolution function is in the bottom figure. For additional explanation, see the text.

FIG. 2: The calculated and measured INS spectra of o -H₂ in the small cage of sII clathrate hydrate. The top figure shows the stick spectrum, while the one convolved with the instrumental resolution function is in the bottom figure. For additional explanation, see the text.

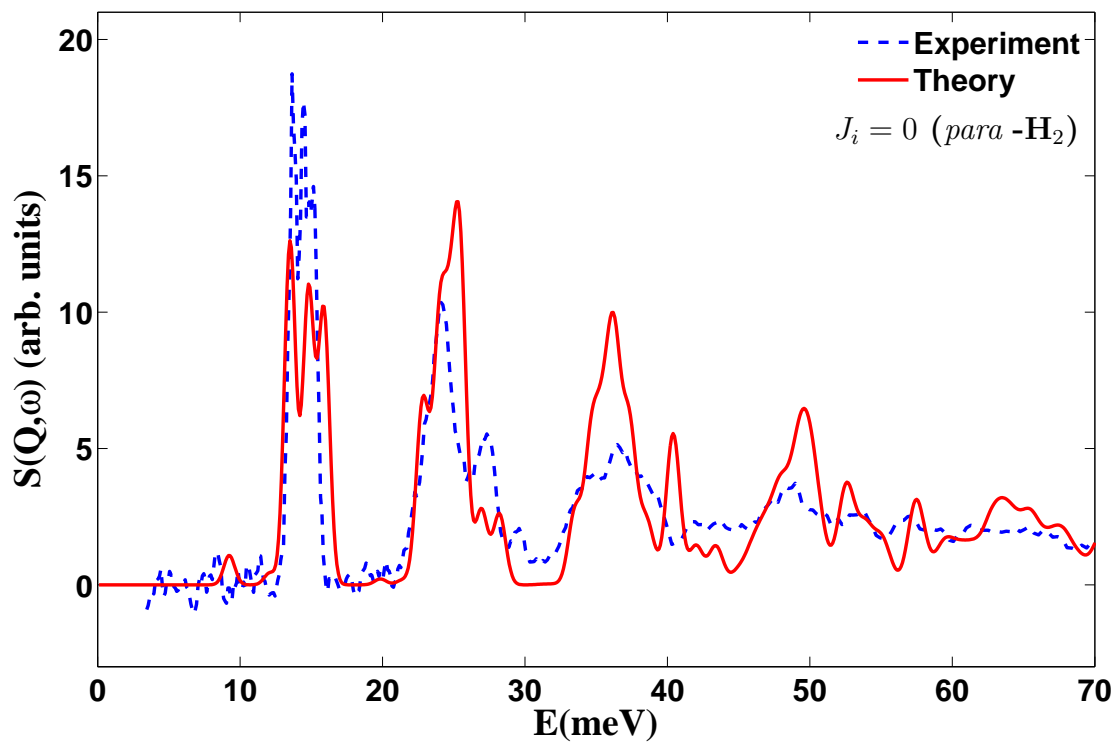
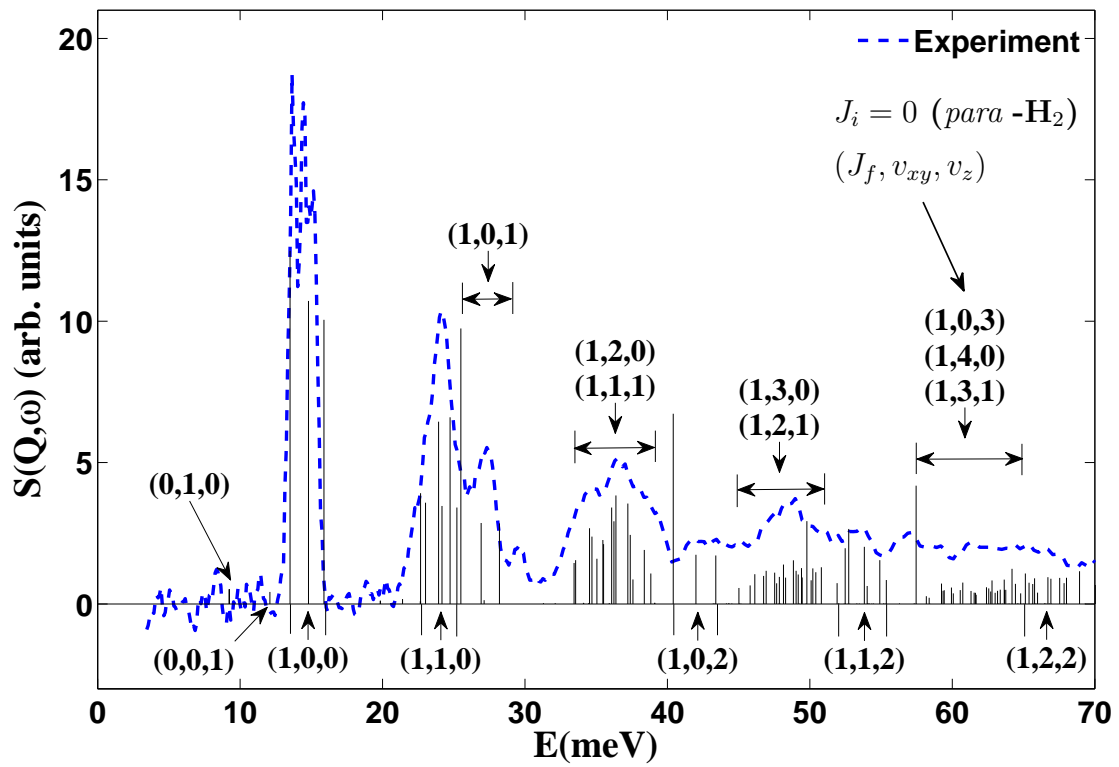


Figure 1 LC13353 18May2011

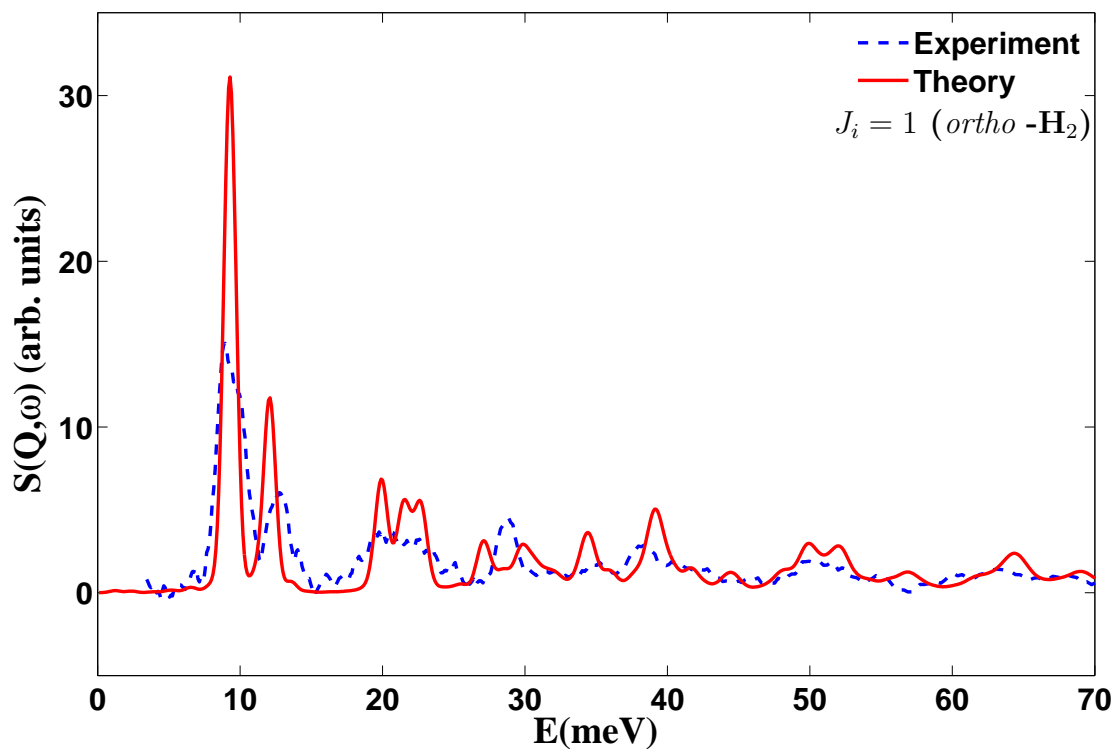
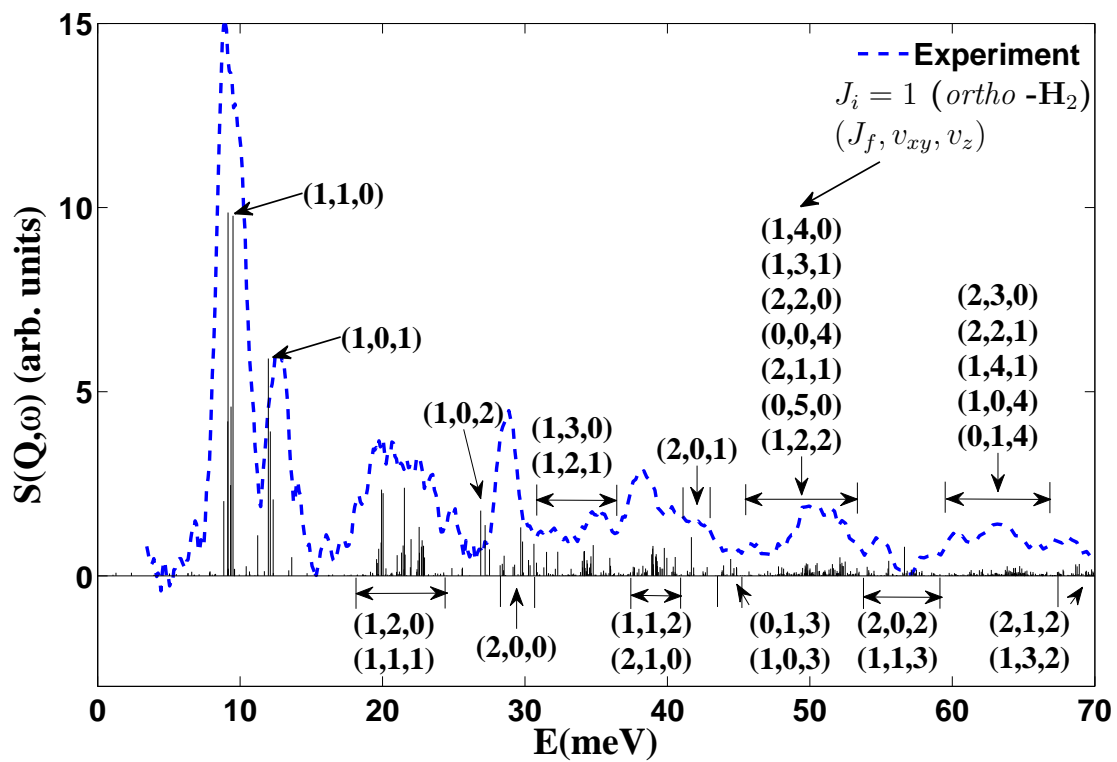


Figure 2 LC13353 18May2011